Science & Technology Development Journal 2024, 27(4):3694-3703

Open Access Full Text Article

Research Article

Surface features of graft-type polymer electrolyte membranes determined by tapping mode atomic force microscopy analysis

Nguyen Nhat Kim Ngan[1,2], Nguyen Manh Tuan[2,3], Nguyen Huynh My Tue[2,3], Vo Thi Kim Yen[2,3], Dinh Tran Trong Hieu[2,3], Hoang Anh Tuan[2,3], Tran Ngoc Tien Phat[2,3], Lam Hoang Hao[2,3], Nguyen Thanh Ta[2,3], Doan Thi Kim Ngan[2,3], Tran Duy Tap[*]

ABSTRACT

Introduction: Polymer electrolyte membrane fuel cells (PEMFCs) are promising renewable energy technologies that are increasingly used in commercial transportation, stationary, and portable devices. In PEMFCs, the surface nature of PEMs plays a key role in the interfacial degradation of membrane–electrolyte assembly and proton conductance and thus strongly impacts the performance and stability of PEMFCs. Consequently, the objective of this work was to investigate the surface features of graft-type poly(styrenesulfonic acid) (PSSA)-grafted poly(ethylene-co-tetrafluoroethylene) polymer electrolyte membranes (ETFE-PEMs) by tapping mode atomic force microscopy (TM-AFM). **Methods:** ETFE-PEMs were prepared via preirradiation-induced grafting of styrene onto an ETFE film followed by sulfonation. All the ETFE-PEMs and their precursor films (original ETFE and polystyrene (PS)-grafted ETLEs) were characterized via TM-AFM. **Results:** In the grafting and sulfonation process, partially grafted PS and PSSA chains accumulate on the sample surface at a low grafting degree (GD) of 21%, and more graft chains diffuse into the bulk of the membranes at higher GDs of 36 and 57%. The polystyrene grafts are immiscible mostly with the amorphous phase of the pristine ETFE film, leading to the formation of a new amorphous phase containing only PS grafts. Sulfonation resulted in microphase separation between the backbone of ETFE and the side chain of PSSA, but the final surface morphology of the membranes can be determined at the grafting step. **Conclusions:** The surface morphology characteristics are more or less ascertained during the grafting process but not during the sulfonation process. The PSSA grafts of ETFE-PEMs are dispersed on the membrane surface, favoring the connection of ionic domains and leading to an increase in proton conductance on the membrane surface. These findings suggest that ETFE-PEMs have advantages in terms of membrane–electrode interfacial properties for PEMFC applications because of their low accumulated surface area and low GD.

Key words: ETFE-PEM, polymer electrolyte membranes, surface feature, AFM

[1]*Faculty of Physics and Engineering Physics, University of Science, Ho Chi Minh City, Vietnam*

[2]*Viet Nam National University, Ho Chi Minh City, Vietnam*

[3]*Faculty of Materials Science and Technology, University of Science, Ho Chi Minh City, Vietnam*

Correspondence

Tran Duy Tap, Email: tdtap@hcmus.edu.vn

History

- Received: 2024-09-30
- Revised: 2024-12-11
- Accepted: 2024-12-25
- Published Online: 2024-12-31

DOI :

https://doi.org/10.32508/stdj.v27i4.4370

INTRODUCTION

The polymer electrolyte membrane fuel cell (PEMFC) has attracted much attention for applications in transportation, stationary, and portable devices because of its high energy efficiency (40–60%) and lack of gas emission. This application is expected to address pollutant emissions and thus reduce the impact of climate change[1]. The polymer electrolyte membrane (or proton exchange membrane) (PEM) is the key component of a PEMFC because its ionic conductivity, mechanical strength, and thermal and chemical stability are significantly related to the performance and durability of the cell. Perfluorosulfonic acid membranes such as Nafion are the state-of-the-art advanced materials for PEMs, but their limitations, such as high production cost and low performance at high temperature and low relative humidity (RH), have triggered investigations of alternative polymer electrolyte membranes to replace Nafion[1]. In our previous works[2–18], we reported the synthesis and characterization of poly(styrenesulfonic acid)-grafted poly(ethylene-co-tetrafluoroethylene) polymer electrolyte membranes (ETFE-PEMs) within a wide range of grafting degrees (GDs) of 0–125%, corresponding to an ion exchange capacity (IEC) of 0–3.3 mmol/g via gamma-ray irradiation-induced grafting of styrene onto an ETFE film (grafted-ETFE) and subsequent sulfonation of the grafted film. Compared with other fully or partially fluorinated graft-type PEMs[19–21] or Nafion membranes[9,10,15,16], ETFE-PEMs exhibit higher or comparable proton conductivities, mechanical integrity and thermal stability. In particular, ETFE-PEMs with high IECs (> 2.7 mmol/g) show greater conductivity at 30% RH and competitive tensile strength at 100% RH and 80 °C than the commercial Nafion-212 membrane[15].

Cite this article : Ngan N N K, Tuan N M, Tue N H M, Yen V T K, Hieu D T T, Tuan H A, Phat T N T, Hao L H, Ta N T, Ngan D T K, Tap T D. **Surface features of graft-type polymer electrolyte membranes determined by tapping mode atomic force microscopy analysis**. *Sci. Tech. Dev. J.* 2024; 27(4):3694-3703.

Recently, membrane–electrode assembly (MEA) failures have been observed after only a few hundred PEM operations and have been found to be closely related to the nature of the membrane surface[22,23]. The inferior interfacial properties of MEAs have been recognized to be associated with backbone and functional chain degradation and crack development. For example, concentrated PSSA grafts on the surface of poly(styrene sulfonic acid) (PSSA)-grafted poly(tetrafluoroethylene-coperfluorovinyl ether) polymer electrolyte membranes (PFA-PEMs) and PSSA-grafted poly(tetrafluoroethylene) polymer electrolyte membranes (PTFE-PEMs) were observed to decompose within 50 h in fuel cells running[24–26]. Moreover, the low or high functional graft distribution on the membrane surface resulted in low conductance and surface fractures, respectively[27,28]. However, there are still limitations in the detailed and systematic evaluation of the surface features of ETFE-PEMs[2,5], although these limitations are quite important for their performance in PEMFCs.

Tapping mode atomic force microscopy (TM-AFM) is a potential method for investigating the surface morphology of membranes because it allows us to observe high-resolution topographic images and avoid any surface dragging effects of tips on surface sampling[29]. In TM-AFM analysis, common parameters such as surface roughness (S_a), root-mean-square roughness (S_q), and maximum spike-to-valley height roughness ($S_z(P\text{-}V)$) are often used to describe the surface architecture in the vertical dimension. Since these parameters do not show any information in the horizontal direction, the additional shape parameter of skewness (S_{kew}) is chosen to provide missing information in the horizontal direction. This combination provides a comprehensive understanding of the surface architecture of membranes. The aim of this work was to investigate the change in the surface morphology of ETFE-PEMs through the preparation procedure and with the degree of grafting via AFM analysis. As the structural features of the final polymer electrolyte membrane (ETFE-PEM) are highly dependent on those of the pristine polymer and grafted polymer films, TM-AFM measurements of the pristine ETFE and grafted-ETFE films were also conducted.

EXPERIMENTAL

Materials

Commercial 50-μm-thick ETFE films (or Tefzel films) were purchased from AGC Ltd., Japan. Furthermore, other chemical substances (i.e., styrene, 1,2-dichloroethane, hydrogen peroxide, acetone, toluene, and chlorosulfonic acid) were obtained from Wako Pure Chemical Industries, Ltd., Japan. In this work, all the chemical substances were used as received (i.e., without further treatment).

Preparation of graft-type ETFE-PEMs

The general procedures for the preparation and chemical structures of ETFE, grafted-ETFE, and ETFE-PEM are depicted in Scheme 1. The preparations were similar to those comprehensively described in our previous works[11,15]. Accordingly, the present study is briefly outlined as follows. The ETFE films were irradiated by g-rays emitted from a Co^{60} source under and an argon atmosphere. The energies of the gamma rays are approximately 1.17 and 1.33 MeV. These energies are high enough for the occurrence of photoelectric, Compton, and pair production effects within the irradiated ETFE films at the same time. These effects can generate a large number of secondary electrons, which in turn induce many sequential physical interactions (coastal interactions) to create free radicals. The absorbed dose and dose rate were 15 kGy and 15 kGy/h, respectively. This irradiation dose is expected to generate free radicals but does not modify the microstructures within the irradiated films[4]. These free radicals serve as active sites for the grafting process. The irradiated films were then immersed in a styrene/toluene mixture at different concentrations and different time courses at 60 °C for graft polymerization to obtain polystyrene-grafted ETFE films. During the grafting process, the PS chains are expected to diffuse through the amorphous phase until the grafting occurs mostly at the crystalline–amorphous interfaces (where the free radicals can last much longer than those in the amorphous regions, where the free radicals vanish rapidly). The degree of grafting (GD) is determined via the following formula: GD (%) = 100*(W_g - W_0)/W_0, where W_0 and W_g are the masses of the sample before and after the grafting step, respectively. The grafted films were soaked in a 0.2 M chlorosulfonic acid solution in 1,2-dichloroethane at 50 °C (approximately 6 hours) for sulfonation to obtain the graft-type ETFE-PEMs[11,15]. Note that the chemical structures of the grafted ETLs and ETFE-PEMs were confirmed by Fourier transform infrared (FT-IR) spectroscopy[11] and X-ray photoelectron spectroscopy (XPS) analysis[5]. Specifically, new bands appeared at 1492 and 1600 cm^{-1} (skeletal in-plane deformation of the conjugated C=C of the benzene ring), and new bands emerged at 756 and 698 cm^{-1} (CH out-of-plane vibration), indicating that styrene was grafted onto the ETFE film. Moreover,

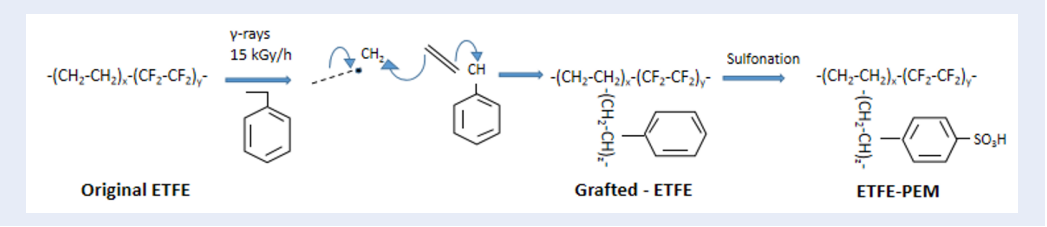

Scheme 1: **Preparation procedure and structures of graft-type ETFE-PEMs.** The samples were prepared via preirradiation-induced grafting of styrene onto the ETFE substrate to obtain the grafted-ETFE and subsequent sulfonation to obtain the ETFE-PEM. Owing to the high energy of gamma rays, the whole volume of the ETFE film is expected to be irradiated at the same time. The generated radicals within the amorphous phase vanish quickly, whereas those within the crystallites or crystallite surfaces can last for a long time. Thus, the grafting is assumed to be at the amorphous–crystalline interface[9,17].

new bands at 840 and 607 cm^{-1} (stretching vibration of S=O) appear after sulfonation, which suggests that the grafted-ETFE was sulfonated successfully to create the ETFE-PEM. XPS analysis revealed a significant decrease in the fluorine content, which mainly resulted from graft incorporation and the defluorination reaction during the grafting process. In addition, an additional peak at 169.1 eV was observed, indicating the existence of sulfonic acid groups (SO_3^-) within the ETFE-PEM.

AFM measurement

The AFM analyses of the original ETFE, grafted-ETFE films, and ETFE-PEMs were carried out with a SPA-400 instrument (Seiko Instruments, Japan) in tapping mode under ambient conditions. The microscope was equipped with a calibrated 20-μm-xy-scan range and a 10-μm-z-scan range of the PZT scanner. All measurements were conducted at room temperature using an aluminum-coated silicon tip (SI-DF40) on a cantilever with a spring constant and resonance frequencies of 31 N/m and 320 Hz, respectively. Surface scanning was performed at a scan rate of 1 Hz. The end radius of the silicon probe was approximately 10 nm. The distance from the probe to the sample was 100 nm. Before the measurement, the samples were cut into small pieces of 1 × 1 cm^2, fixed to the mica substrate with adhesive tape, and then mounted onto the sample holder. In this study, all the images were analyzed via Gwyddion software (version 2.49) to determine the specific roughness parameters (i.e., S_a, S_q, S_z(*P-V*), and S_{kew}) of the surface morphology. These values were determined directly via integrated routines from the height scan. S_a describes the mean height of asperities (i.e., average surface roughness), whereas S_q represents the standard deviation of a height profile from its average height (root mean squared surface roughness)[30,31]. Both the S_a and S_q parameters describe the vertical dimensions quite well but provide no insight into the horizontal dimensions of the surface architecture. S_z(*P-V*)) and S_{kew}, which represent the distance from the highest to the lowest points and the irregularities on the surface, are also used to evaluate the overall roughness and asymmetry of the topography. Accordingly, the S_z(*P-V*)) and S_{kew} parameters are more descriptive in horizontal dimensions. The line profile was generated by selecting one line from the corresponding two-dimensional image and subsequently plotting x-translation versus height data (z-axis). Each profile was plotted by using an appropriate height scale to provide optimum resolution. These parameters are calculated through the following expressions[32]:

$$S_a = \frac{1}{L}\int_0^L |z_i - \bar{z} \tag{1}$$

$$S_q = \left[\frac{1}{L}\int_0^L (z_i - \bar{z})^2\, dx\right]^{1/2} \tag{2}$$

$$S_z\,(P-V) = |maxZz + minZz| \tag{3}$$

$$S_{kew} = \frac{1}{LS_q^3}\int_0^L (z_i - \bar{z})^3\, dx \tag{4}$$

where L is the sampling length, z_i is the height value of point i, and $\bar{z}$ is the average height within the scanning area. The height distribution, r(z), is also plotted as the normalized probability of finding a particular height z with the origin at the lowest observed z–height[33]. The distribution of surface height ρ(z) is described in the following form:

$$\rho\,(z) = \left(1/S_q\sqrt{2\pi}\right) exp\left[-(z-\bar{z})^2/2S_q^2\right] \tag{5}$$

RESULTS

The surface features through the preparation procedure

Figure 1 (a-i) and Table 1 show the typical 2D and 3D images and height profiles of the original ETFE, grafted-ETFE, and ETFE-PEM at a GD of 21% and their corresponding surface parameters. Obviously, the Sa S_a value of the original-ETFE (15.5 nm) is greater than that of the grafted-ETFE (8.0 nm) and ETFE-PEM (10.1 nm). The 2D and 3D images also exhibit the same result. Moreover, bright yellow regions corresponding to the softer domains (amorphous regions) are dominant over harder domains (crystallite regions) for the three samples. The straight lines in the 2D images in Figure 1(d-f) represent the positions of the surface roughness profiles, as shown in Figure 1(g-i). As shown in the figures, the surface roughness profiles of the grafted-ETFE and ETFE-PEM films are more relatively homogeneous than those of the pristine ETFE film. The maximum surface heights S_z(*P-V*) of the original-ETFE, grafted-ETFE, and ETFE-PEM are 104.9, 72.2, and 81.0 nm, respectively (Table 1). Moreover, their root mean square roughness values (S_q) and Skew $_{values}$ are 19.6, 10.0, and 12.6 nm and 0.6, 0.3, and 0.1, respectively. All the values of the above surface parameters of the grafted-ETFE and ETFE-PEM films are lower than those of the pristine ETFE film.

Surface features with various degrees of grafting

Grafted ETLEs

Figure 2 shows 3D AFM images of grafted-ETFE films with different GDs ranging from 0–57%. As the degree of grafting increases, the formation of small graft domains containing polystyrene (PS) chains increases but at a lower rate. The S_a values at GDs of 21, 36, and 57% are 15.5, 8.0, 5.9, and 8.2 nm, respectively. With similar grafting degrees, the values of S_q (10.0, 7.6, and 10.1 nm), S_z(*P-V*) (72.2, 71.8, 73.6) and S_{kew} (0.3, 0.6, and 0.5) are obtained. Clearly, all surface parameters of the grafted-ETFE films are lower than those of the pristine ETFE film, as shown in Table 2.

ETFE-PEMs

Figure 3 and Table 3 present 3D AFM images of ETFE-PEMs with GDs of 21-57% and the corresponding surface parameters. After sulfonation, the membranes exhibit phase separation between the hydrophobic domain (ETFE-based film) and the hydrophilic domain possessing groups of ionic clusters (PSSA) [9,10,15,16]. As a result, the connection of ionic domains increases with the degree of grafting. At the same time, larger continuous domains are formed, especially at GDs of 36 and 57% [10]. The S_a values at GDs of 21, 36, and 57% are 10.1, 14.2, and 23.3 nm, respectively. With similar grafting degrees, the values of S_q (12.6, 16.4, and 28.3), S_z(*P-V*) (81.0, 81.4, and 169.1) and S_{kew} (0.1, 0.1, and 0.2) are obtained. All surface parameters at GDs of 21 and 36% are lower than those of the pristine ETFE film, whereas those at a GD of 57% are greater.

Figure 4 depicts the height distributions of the original ETFE, grafted-ETFE, and ETFE-PEM with GDs of 21-57% at a scan size of 2000 nm. The height distribution of the original ETFE is displayed by a red line, whereas those of the grafted-ETFE films and ETFE-PEMs are represented by cyan and green lines. The height distribution of the pristine film can be fitted by two Gaussian peaks with average heights of 40.1 and 72.8 nm and FWHMs of 35.7 and 9.4 nm. In contrast, the height distributions of the grafted-ETFE films at GDs of 21, 36, and 57% can be fitted by only one Gaussian peak with average heights of 24.9, 22.5, and 22.4 nm and FWHMs of 21.4, 16.4, and 16.3 nm, respectively. As expected, the z values of the grafted-ETFE films are lower than those of the original ETFE film, i.e., similar to the case of S_a indicated in Table 2. The height distribution of the ETFE-PEM at a GD of 21% can be fitted by a single Gaussian peak with an average height of 38.9 nm and an FWHM of 30.4 nm. For the ETFE-PEMs at higher GDs, the height distribution can be fitted by two Gaussian peaks with average heights of 30.1 and 56.7 nm and FWHMs of 18.7 and 21.8 nm for a GD of 36% and average heights of 70.5 and 108.7 nm and FWHMs of 41.0 and 27.8 nm for a GD of 57%. Interestingly, the z values of all the ETFE-PEMs are greater than those of the grafted-ETFE films. All the height distributions fit relatively high values of R^2 (> 0.85), as displayed in Table 4. Note that in the case of the pristine ETFE, the three-peak model was also fitted with the experimental height distribution, but the third peak was very small in peak area and FWHM. This small peak area and small FWHM value are not suitable for any component of the surface architecture in the pristine film. A similar situation is found for the case of the grafted-ETFE with a GD of 57%. Specifically, a two-peak model was also fitted with the experimental height distribution, but the second peak was very small in peak area and FWHM value. This very small peak area and very small FWHM value do not correspond to any component of the surface architecture in the grafted ETLE film.

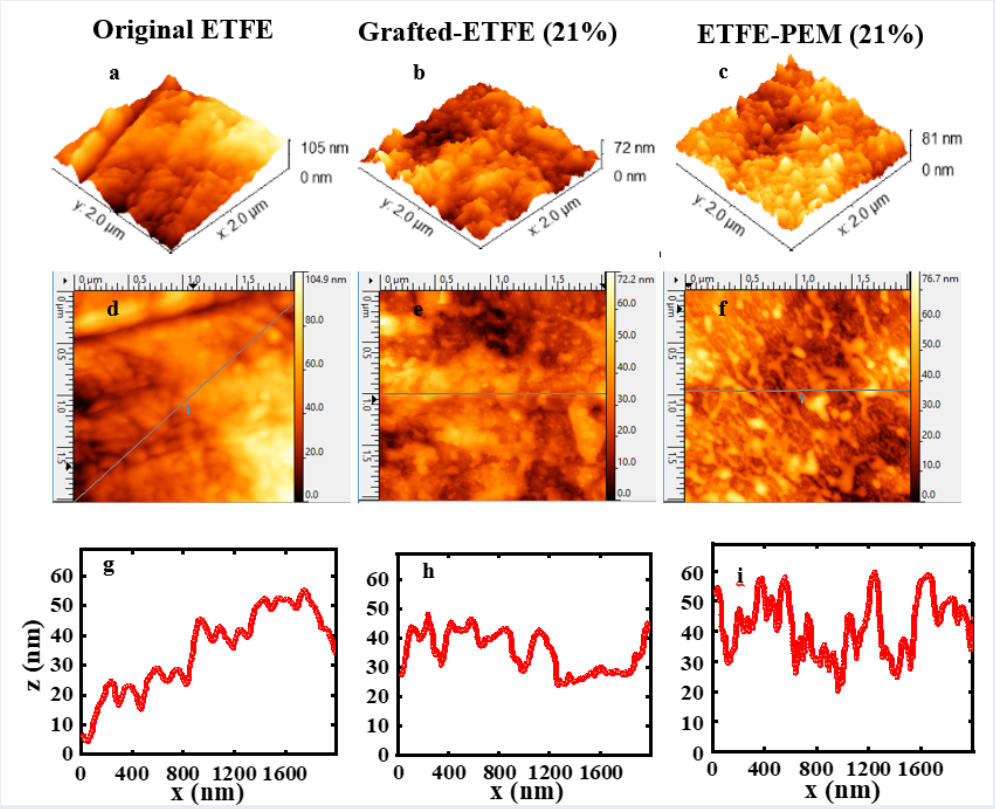

Figure 1: **Surface features obtained through the preparation procedure at a scan size of 2000 nm.** 3D (a-c) and 2D (d-f) AFM images and line profiles (g-i) of the original ETFEs, grafted-ETFEs, and ETFE-PEMs with a GD of 21%. The surface roughness profiles of the grafted-ETFE and ETFE-PEM films are more homogeneous than those of the original ETFE film.

Table 1: Specific roughness parameters (S_a, S_q, S_z(*P-V*), and S_{kew}) of the original ETFE, grafted-ETFE and ETFE-PEM with a GD of 21%. The surface parameters of the grafted-ETFE and ETFE-PEM films are lower than those of the pristine ETFE film.

Sample	GD (%)	S_a (nm)	S_q (nm)	S_z(P-V) (nm)	S_{kew}
Original ETFE	0	15.5	19.6	104.9	0.6
Grafted-ETFE	21	8.0	10.0	72.2	0.3
ETFE-PEM	21	10.1	12.6	81.0	0.1

Table 2: Specific roughness parameters (S_a, S_q, S_z(*P-V*), and S_{kew}) of the grafted-ETFE films with GDs of 0 - 57%. The surface parameters of the grafted films are all lower than those of the pristine ETFE film. Here, the specific roughness parameters of the original ETFE are represented again for comparison.

Sample	GD (%)	S_a (nm)	S_q (nm)	S_z(P-V) (nm)	S_{kew}
Original ETFE	0	15.5	19.6	104.9	0.6
Grafted-ETFE	21	8.0	10.0	72.2	0.3
Grafted-ETFE	36	5.9	7.6	71.8	0.6
Grafted-ETFE	57	8.2	10.1	73.6	0.5

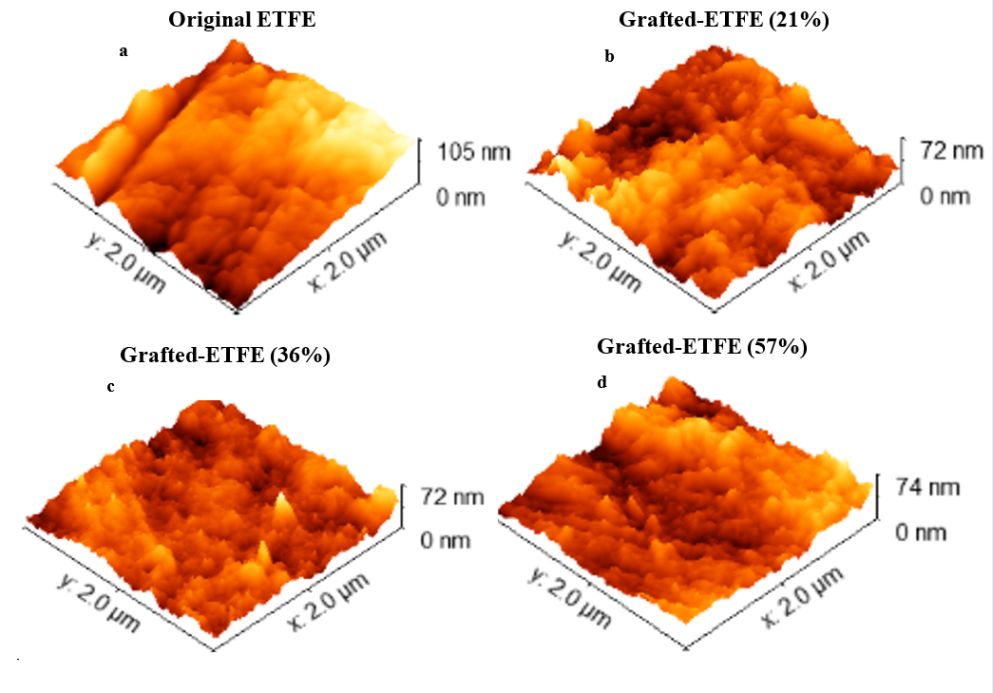

Figure 2: **3D surface images of the grafted-ETFE films with GDs of 0- 57% at a scan size of 2000 nm.** The bright yellow regions correspond to the softer domains of the amorphous regions of the pristine ETFE and/or PS grafts. Note that the image of the original ETFE is represented again for comparison.

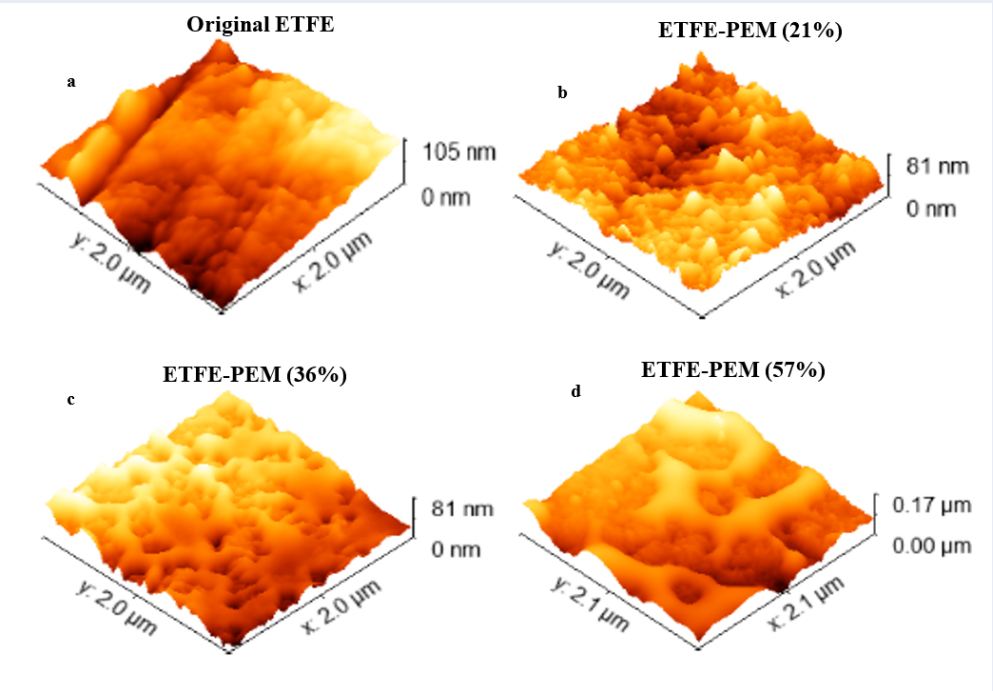

Figure 3: 3D surface images of the ETFE-PEMs with GDs of 0-57% at a scan size of 2000 nm. The connections among ionic domains on the membrane surface increase with the degree of grafting. In this case, the 3D image of the pristine film is also represented again for comparison.

Table 3: Specific surface parameters (S_a, S_q, S_z(*P-V*), and S_{kew}) of the ETFE-PEMs with GDs of 0 - 57%. The surface parameters of the ETFE-PEMs at GDs of 21 and 36% are lower than those of the pristine ETFE film. For comparison, the specific roughness parameters of the original film are also represented again.

Sample	GD (%)	S_a (nm)	S_q (nm)	S_z(P-V) (nm)	S_{kew}
Original ETFE	0	15.5	19.6	104.9	0.6
ETFE-PEM	21	10.1	12.6	81.0	0.1
ETFE-PEM	36	14.2	16.4	81.4	0.2
ETFE-PEM	57	23.3	28.3	169.1	0.2

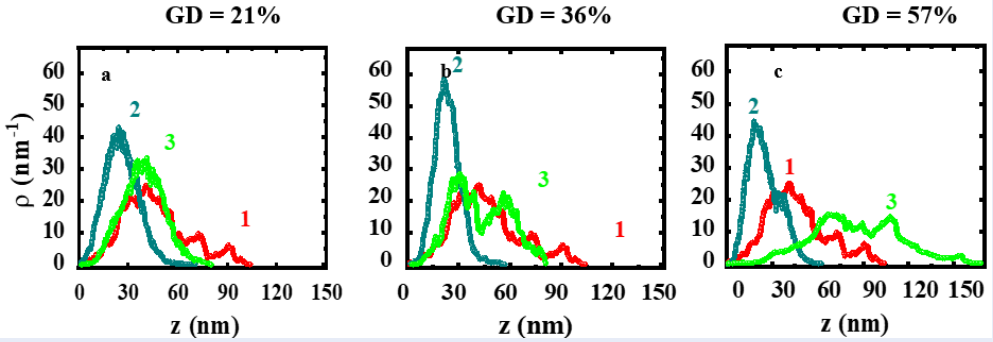

Figure 4: The height distribution of the samples at a scan size of 2000 nm. The original ETFE (1 – red line), grafted-ETFE (2 – cyan line), and ETFE-PEM (3 – green line) have GDs of 21–57%.

Table 4: Specific surface parameters (z and FWHM) of the original ETFE, grafted-ETFE, and ETFE-PEMs with GDs ranging from 21–57%. The z values of the grafted-ETFE films slightly decrease with GD, whereas those of the ETFE-PEMs increase with GD.

Sample	GD (%)	z (nm)	FWHM (nm)	R^2
Original ETFE (peak 1)	0	40.1	35.7	0.932
Original ETFE (peak 2)	0	72.8	9.4	0.932
Grafted-ETFE	21	24.9	24.1	0.983
Grafted-ETFE	36	22.5	16.4	0.987
Grafted-ETFE	57	22.4	16.3	0.857
ETFE-PEM	21	38.9	30.4	0.985
ETFE-PEM (peak 1)	36	30.1	18.7	0.942
ETFE-PEM (peak 2)	36	56.7	21.8	0.942
ETFE-PEM (peak 1)	57	70.5	41.0	0.927
ETFE-PEM (peak 2)	57	108.7	27.8	0.927

DISCUSSIONS

The results presented in Figure 1 and Table 1 indicate that grafting and sulfonation induced significant changes in the surface features of the grafted ETLEs and ETFE-PEMs. Partially grafted PS and PSSA chains accumulate on the sample surface at a low GD of 21%. In other words, the surface features observed in Figure 1 and Table 1 reflect the partial presence of the graft chains, which are more homogeneously distributed than those of the pristine film. This result can be explained by the fact that the introduced PS chains were mostly immiscible with the amorphous phase of the pristine ETFE film, leading to the formation of a new amorphous phase containing only PS grafts[5,8–10]. Sulfonation results in microphase separation between the backbone of ETFE and the side chain of PSSA, but the final membrane morphology can be determined at the grafting step[12,16,17]. Accordingly, the surface parameters of the grafted-ETFE and ETFE-PEM (GD = 21%), represented in Table 1, are quite similar. In the case of the grafted-ETFE films, all surface parameters shown in Table 2 are lower than those of the pristine ETFE film because of the immiscibility between the PS grafts and the amorphous phase of the ETFE-based film, as mentioned above. In addition, the surface parameters do not increase with the GD, indicating that some of the PS grafts diffused into the bulk of the ETFE at the higher GD[5]. In particular, the S_a, S_q, and $S_z(P\text{-}V)$ parameters (Table 2) decrease with increasing GD from 0 to 36% and then increase again at a higher GD of 57%. This phenomenon should be related to the changes in lamellar structures reported previously[16,17]. Specifically, the lamellar period increases quickly from 19.1 to 25.4 nm, increases slowly from 25.4 to 28.5 nm, and then remains unchanged at approximately 28 nm within the GDs of 0–19%, 19–59%, and 59–117%, respectively. In other works, at a GD of approximately 57%, most of the graft chains were introduced out of the lamellar structures, leading to more accumulation of graft chains on the film surface, resulting in increases in the S_a, S_q, and $S_z(P\text{-}V)$ parameters. For the case of ETFE-PEMs, all surface parameters (S_a, S_q, and $S_z(P\text{-}V)$) shown in Table 3 are lower than those of the pristine ETFE film and grafted-ETFE films displayed in Table 2. In contrast, the values of S_{kew} for the ETFE-PEMs are lower than those for the grafted-ETFE films. Furthermore, the surface parameters (Table 3) increase with the degree of grafting, i.e., a trend dissimilar to that of the grafted ETLEs (Table 2). This result reflects the effects of microphase separation, as discussed above[10]. In particular, the surface parameters at the GD of 57% are significantly greater than those at the GDs of 0, 21, and 36%. This phenomenon can be elucidated similarly to that of the grafted-ETFEs at a GD of 57%. Specifically, at a GD of approximately 57%, most of the PSSA chains were generated from the lamellar stacks, leading to more accumulation of PSSA chains on the film surface, resulting in an increase in the phase separation and values of S_a, S_q, $S_z(P\text{-}V)$, and *the skew* parameters[16,17].

The results of the height distribution shown in Figure 4 and Table 4 indicate that the PS grafts of the grafted-ETFE films are mostly immiscible within the ETFE-based matrix and can be described as a single distribution (i.e., homogeneous distribution). Moreover, the decreases in the average height (24.9–22.4 nm) and FWHM (21.1–16.3 nm) with increasing degree of grafting suggest that more PS chains diffused into the bulk of the grafted-ETFE films. This phenomenon is consistent with the 3D image features shown in Figure 2(b-d). In contrast, the PSSA grafts of ETFE-PEMs are dispersed on the membrane surface, leading to an increase in the FWHM values (Table 4). These dispersed aggregates are favorable for the connection of ionic domains, leading to larger continuous ionic domains, as observed in the 3D image features (Figure 3(b-d)). In other words, the dispersed distribution of PSSA grafts can accelerate the conductance on the membrane surface[5].

CONCLUSIONS

The surface features of the ETFE-PEMs obtained through the preparation procedure and with different degrees of grafting were investigated via TM-AFM analysis. Partially grafted PS and PSSA chains accumulated on the sample surface at a low GD of 21% and then diffused partially into the bulk of the membranes at higher GDs of 36 and 57%. All the surface parameters of the grafted-ETFE films did not clearly change with GD, whereas those of the ETFE-PEMs increased with GD. In particular, the PS grafts of the grafted-ETFE films are mostly immiscible within the ETFE-based matrix and can be described as having a single distribution (i.e., homogeneous distribution). In contrast, the PSSA grafts of ETFE-PEMs are dispersed on the membrane surface, favoring the connection of ionic domains and leading to larger continuous ionic domains. The dispersed distribution of PSSA grafts can accelerate proton conductance on the membrane surface, while the low accumulation of grafts on the membrane surface at a low GD is advantageous for improving the membrane–electrode interfacial properties of PEMFCs.

LIST OF ABBREVIATIONS

AFM: Atomic force microscopy
ETFE: Ethylene-co-tetrafluoroethylene
ETFE-PEM: Poly(styrenesulfonic acid)-grafted poly(ethylene-co-tetrafluoroethylene) polymer electrolyte membrane
FWHM: Full width at half maximum
GD: Grafting degree
Grafted-ETFE: Polystyrene-grafted ethylene-co-tetrafluoroethylene
IEC: Ion exchange capacity
PEMCF: Polymer electrolyte membrane fuel cell
PS: Polystyrene
PSSA: Poly(styrenesulfonic acid)
RH: Relative humidity
TM-AFM: tapping mode atomic force microscopy

COMPETING INTERESTS

There are no conflicts of interest to declare.

ACKNOWLEDGMENTS

This work was funded by the Vingroup Big Data Institute (VINBIGDATA), Vingroup and supported by the Vingroup Innovation Foundation (VINIF) under project code VINIF.2020.DA08.

DATA AVAILABILITY STATEMENT

The data sets are not publicly available but are available from the corresponding author upon reasonable request.

AUTHORS CONTRIBUTION

Tran Duy Tap: Conceptualization, project administration, funding acquisition, supervision, resources, investigation, methodology, data curation, formal analysis, supervision, validation, visualization, writing - original draft, writing - review & editing. **Nguyen Nhat Kim Ngan**: Investigation, methodology, data curation, formal analysis, validation, visualization, writing - original draft, writing - review & editing. **Nguyen Manh Tuan, Nguyen Huynh My Tue, Vo Thi Kim Yen, Dinh Tran Trong Hieu, Hoang Anh Tuan, Tran Ngoc Tien Phat, Lam Hoang Hao, Nguyen Thanh Ta, Doan Thi Kim Ngan**: Investigation, Formal analysis, Visualization, Validation.

REFERENCES

1. Smitha B, Sridhar S, Khan AA. Solid polymer electrolyte membranes for fuel cell applications - A Review. Journal of Membrane Science. 2005;259(1-2):10-26;Available from: https://doi.org/10.1016/j.memsci.2005.01.035.
2. Hao LH, Hieu DTT, Danh TT, Long TH, Phuong HT, Luan LQ, Man TV, Tuyen LA, Ngoc PK, Tap TD. Surface features of polymer electrolyte membranes for fuel cell applications: An approach using S2p XPS analysis. Science & Technology Development Journal. 2021; 24(3):2100-2109;Available from: https://stdj.scienceandtechnology.com.vn/index.php/stdj/article/view/2556.
3. Hao LH, Hieu DTT, Long TH, Hoa DV, Danh TT, Man TV, Luan LQ, Phuong HT, Hong PTT, Tap TD. Investigation of the lamellar grains of graft-type polymer electrolyte membranes for hydrogen fuel cell application using ultrasmall-angle X-ray scattering. VNU Journal of Science: Natural Sciences and Technology. 2021;37:1-9;Available from: https://doi.org/10.25073/2588-1140/vnunst.5216.
4. Hao LH, Hieu DTT, Luan LQ, Phuong HT, Phuc DV, Tuyen LA, Hong PTT, Man TV, Tap TD. Electron and gamma irradiation-induced effects in poly(ethylene-co-tetrafluoroethylene) films. Journal of Applied Polymer Science. 2022;139(29):1-18;Available from: https://onlinelibrary.wiley.com/doi/10.1002/app.52620.
5. Hao LH, Tap TD, Hieu DTT, Korneeva E, Tiep NV, Yoshimura K, Hasegawa S, Sawada S, Man TV, Hung NQ, Tuyen LA, Phuc DV, Luan LQ, Maekawa Y. Morphological characterization of grafted polymer electrolyte membranes at a surface layer for fuel cell application. Journal of Applied Polymer Science. 2022;139(14):51901;Available from: https://doi.org/10.1002/app.51901.
6. Hieu DTT, Hao LH, Danh TT, Luan LQ, Man TV, Phuong HT, Phuc DV, Tuyen LA, Ngoc PK, Tap TD. Investigation of the water states of poly(styrene sulfonic acid) (PSSA) grafted poly(ethylene-co-tetrafluoroethylene) copolymer using FT-IR analysis, Vietnam Journal of Science, Technology and Engineering. 2022;64:3-9;Available from: https://doi.org/10.31276/VJSTE.64(2).03-09.
7. Hieu DTT, Hao LH, Long TH, Tien VV, Cuong NT, Man TV, Loan TTH, Tap TD. Investigation of chemical degradation and water states in the graft-type polymer electrolyte membranes. Polymer Engineering and Science. 2022;62: 2757–2768;Available from: https://doi.org/10.1002/pen.26059.
8. Long TH, Hieu DT, Hao LH, Cuong NT, Loan TTH, Man TV, Tap DT. Positron annihilation lifetime spectroscopic analysis of Nafion and graft-type polymer electrolyte membranes for fuel cell application. Polymer Engineering and Science. 2022;62:4005-4017;Available from: https://doi.org/10.1002/pen.26162.
9. Tap TD, Long TH, Hieu DT, Hao LH, Phuong HT, Luan LQ, Mann TV. Positron annihilation lifetime study of subnano level free volume features of grafted polymer electrolyte membranes for hydrogen fuel cell applications. Polymers for Advanced Technologies. 2022;33:2952-2965;Available from: https://doi.org/10.1002/pat.5761.
10. Tap TD, Hasegawa S, Yoshimura K, Yen VTK, Tue NH, Tuan NM, Hieu DTT, Tuan HA, Hao LH, Nguyen LL, Phuong HT, Luan LQ, Man TV, Maekawa Y. Phase separation and water channels in graft-type polymer electrolyte membranes for hydrogen fuel cell. International Journal of Hydrogen Energy. 2024;59:777-790;Available from: https://doi.org/10.1016/j.ijhydene.2024.02.082.
11. Tap TD, Nguyen LL, Hien NQ, Thang PB, Sawada SI, Hasegawa S, Maekawa Y. Humidity and temperature effects on mechanical properties and conductivity of graft-type polymer electrolyte membrane. Radiation Physics and Chemistry. 2018;151:186-191;Available from: https://doi.org/10.1016/j.radphyschem.2018.06.033.
12. Tuan NM, Tue NH, Yen VTK, Ngan NNK, Hieu DTT, Tuan HA, Huy DQ, Tap TD. Features of ionic domains in graft-type polymer electrolyte membranes using small angle X-ray scattering analysis. Science & Technology Development Journal. 2024;27:1-13;Available from: https://doi.org/10.32508/stdj.v26i4.4052.
13. Tue NHM, Long TH, Hieu DTT, Hao LH, Yen VTK, Tuan NM, Phuong HT, Luan LQ, Hong PTT, Man TV, Tap TD. Effects of source correction in positron annihilation lifetime spectroscopic analysis of graft-type polymer electrolyte membranes. Science & Technology Development Journal. 2023;26:3060-3068;Available from: https://doi.org/10.32508/stdj.v26i4.4052.

14. Yen VTK, Hieu DTT, Hao LH, Long TH, Tue NHM, Tuan NM, Cuong NT, Loan TTH, Man TV, Tap TD. Characterization of graft-type polymer electrolyte membrane at low grafting degree for fuel cell. Science & Technology Development Journal. 2023;26(2):2799-2807;Available from: https://doi.org/10.32508/stdj.v26i2.4051.
15. Tap TD, Sawada SI, Hasegawa S, Katsumura Y, Maekawa Y. Poly (ethylene-co-tetrafluoroethylene)(ETFE)-based graft-type polymer electrolyte membranes with different ion exchange capacities: Relative humidity dependence for fuel cell applications. Journal of Membrane Science. 2013;447:19-25;Available from: https://doi.org/10.1016/j.memsci.2013.07.041.
16. Tap TD, Sawada S, Hasegawa S, Yoshimura K, Oba Y, Ohnuma M, Katsumura Y, Maekawa Y. Hierarchical structure−property relationships in graft-type fluorinated polymer electrolyte membranes using small- and ultrasmall-angle X-ray scattering analysis. Macromolecules. 2014;47(7):2373-2383;Available from: https://doi.org/10.1021/ma500111x.
17. Tap TD, Nguyen LL, Zhao Y, Hasegawa S, Sawada SI, Hung NQ, Maekawa Y. SAXS investigation on morphological change in lamellar structures during propagation steps of graft-type polymer electrolyte membranes for fuel cell applications. Macromolecular Chemistry and Physics. 2020;221(3):1900325;Available from: https://doi.org/10.1002/macp.201900325.
18. Tap TD, Nguyen LL, Hasegawa S, Sawada SI, Luan LQ, Maekawa Y. Internal and interfacial structure analysis of graft-type fluorinated polymer electrolyte membranes by small-angle X-ray scattering in the high q range. Journal of Applied Polymer Science. 2020;137(35):49029;Available from: https://doi.org/10.1002/app.49029.
19. Nagy G, Sproll V, Gasser U, Schmidt TJ, Gubler L, Balog S. Scaling the graft length and graft density of irradiation-grafted copolymers. Macromolecular Chemistry and Physics. 2018;219(21):1800311;Available from: https://doi.org/10.1002/macp.201800311.
20. Sproll V, Schmidt TJ, Gubler L. Grafting design: A strategy to increase the performance of radiation-grafted membranes. Polymer International. 2016;65(2):174-180;Available from: https://doi.org/10.1002/pi.5041.
21. Gürsel SA, Schneider J, Ben Youcef H, Wokaun A, Scherer GG. Thermal properties of proton-conducting radiation-grafted membranes. Journal of Applied Polymer Science. 2008;108(6):3577-3585;Available from: https://doi.org/10.1002/app.27947.
22. Hatanaka T, Hasegawa N, Kamiya A, Kawasumi M, Morimoto Y, Kawahara K. Cell performances of direct methanol fuel cells with grafted membranes. Fuel 2002;81(17):2173-2176;Available from: https://doi.org/10.1016/S0016-2361(02)00164-3.
23. Sherazi TA, Guiver MD, Kingston D, Ahmad S, Kashmiri MA, Xue X. Radiation-grafted membranes based on polyethylene for direct methanol fuel cells. Journal of Power Sources 2010;195(1):21-29;Available from: https://doi.org/10.1016/j.jpowsour.2009.07.021.
24. Nasef MM, Saidi H, Ambar M. Cation exchange membranes by radiation-induced graft copolymerization of styrene onto PFA copolymer films. IV. Morphological investigations using X-ray photoelectron spectroscopy. Journal of Applied Polymer Science. 2000;77:2455;Available from: https://onlinelibrary.wiley.com/doi/abs/10.1002/1097-4628(20000912)77:11%3C2455::AID-APP14%3E3.0.CO;2-5.
25. Nasef MM, Saidi H. Postmortem analysis of Journal of applied polymer science radiation grafted fuel cell membrane using X-ray photoelectron spectroscopy. Journal of New Materials for Electrochemical Systems 2002;5:183;Available from: https://eprints.utm.my/3714/1/Nasef2002_PostmorteAnalysisRadiationGraftedFuel.pdf.
26. Nasef MM, Saidi H, Nor HM, Yarmo MA. XPS studies of radiation grafted PTFE-g-polystyrene sulfonic acid membranes. Journal of applied polymer science 2000;76:336;Available from: https://onlinelibrary.wiley.com/doi/abs/10.1002/(SICI)1097-4628(20000418)76:3%3C336::AID-APP9%3E3.0.CO;2-E.
27. Nasef MM, Saidi H, Nor HM, Foo OM. Proton exchange membranes prepared by simultaneous radiation grafting of styrene onto poly(tetrafluoroethylene-co-hexafluoropropylene) films. II. Properties of sulfonated membranes. Journal of applied polymer science 2000;78:2443;Available from: https://onlinelibrary.wiley.com/doi/abs/10.1002/1097-4628(20001227)78:14%3C2443::AID-APP30%3E3.0.CO;2-E.
28. Gubler L, Prost N, Gürsel SA, Scherer GG. Proton exchange membranes prepared by radiationgrafting of styrene/divinylbenzene onto poly(ethylene-alt-tetrafluoroethylene) for low temperaturefuel cells. Solid State Ionics. 2005;176:2849;Available from: https://www.sciencedirect.com/science/article/abs/pii/S0167273805004686.
29. Giessibl FJ. Advances in atomic force microscopy. Reviews of Modern Physics. 2003;75(3):949;Available from: https://doi.org/10.1103/RevModPhys.75.949.
30. Webb HK, Truong VK, Hasan J, Fluke C, Crawford RJ, Ivanova EP. Roughness parameters for standard description of surface nanoarchitecture. Scanning. 2012;34(4):257-263;Available from: https://doi.org/10.1002/sca.21002.
31. Nečas D, Klapetek P. Gwyddion: an open-source software for SPM data analysis. Central European Journal of Physics. 2012;10(1):181-188;Available from: https://doi.org/10.2478/s11534-011-0096-2.
32. Motegi T, Yoshimura K, Zhao Y, Hiroki A, Maekawa Y. Direct observation and semiquantitative analysis of hierarchical structures in graft-type polymer electrolyte membranes using the AFM technique. Langmuir. 2022;38(32):9992-9999;Available from: https://pubs.acs.org/doi/abs/10.1021/acs.langmuir.2c01398.
33. Spreitzer H, Kaufmann B, Ruzié C, Röthel C, Arnold T, Geerts YH, Teichert C, Resel R, Jones AO. Alkyl chain assisted thin film growth of 2,7-dioctyloxy-benzothienobenzothiophene. Journal of Materials Chemistry C. 2019;7(27):8477-8484;Available from: https://doi.org/10.1039/C9TC01979K.